

INVERSION FOR PHYSICAL CHARACTERISTICS OF SNOW USING PASSIVE RADIOMETRIC OBSERVATIONS

By S. R. ROTMAN, A. D. FISHER, and D. H. STAELIN

(Research Laboratory of Electronics, Massachusetts Institute of Technology, Cambridge, Massachusetts 02139, U.S.A.)

ABSTRACT. The Nimbus-6 Satellite's Scanning Microwave Spectrometer (SCAMS) mapped the terrestrial surface continuously for eleven months at 22.2 and 31.6 GHz. A semi-empirical method was devised to process these observations of Greenland and Antarctica and to infer long-term snow accumulation rates; comparison with *in situ* data suggests the method is generally successful except in certain locations where re-melting is more likely.

RÉSUMÉ. *Les caractéristiques physiques de la neige déduites d'observations radiométriques passives.* Le spectromètre à micro-ondes du satellite d'observation Nimbus-6 (SCAMS) a cartographié la surface de la terre de manière continue pendant onze mois sur deux fréquences (22,2 et 31,6 GHz). On a décrit une méthode semi-empirique pour procéder aux observations pour le Groenland et l'Antarctique et en déduire les taux d'accumulation à long terme. Sa comparaison avec des données recueillies sur place montre que la méthode est souvent fructueuse, sauf en certains points où des phénomènes de fusion se produisent probablement.

ZUSAMMENFASSUNG. *Ermittlung physikalischer Eigenschaften von Schnee mit Hilfe passiver radiometrischer Beobachtungen.* Das Mikrowellen-Abtastspektrometer des Satelliten Nimbus-6 nahm die Erdoberfläche laufend während elf Monaten in den Frequenzen 22,2 und 31,6 GHz auf. Zur Auswertung dieser Beobachtungen über Grönland und Antarktika und zur Ermittlung langfristiger Akkumulationsraten wurde ein halb-empirisches Verfahren entwickelt. Der Vergleich mit Felddaten zeigt, dass die Methode im allgemeinen brauchbar ist, ausser in gewissen Gebieten, wo vermutlich Rückschmelzprozesse stattfinden.

INTRODUCTION

Radiometric observations of snow at microwave frequencies have shown low values of emissivity (0.65–0.9) over the firm of Greenland and Antarctica. Absorption of microwaves by the snow and the emissivity of the air–snow boundary alone do not properly explain these results unless volume scattering of radiation by the snow medium is included (Kunzi and others, 1976). Models explaining the scattering properties of the snow have been developed by several researchers. Chang and others (1976), Zwally (1977), and Tsang and Kong (1977) modeled the snow as spherical crystals and calculated the Rayleigh and Mie scattering. Tsang and Kong (1975, 1976) and Fisher (1977) have analyzed scattering based on one-dimensional (laminar) and three-dimensional statistically stationary and non-stationary refractive-index fluctuations. Since the scattering and absorption of the snow are functions of its temperature, density, and particle size, the physical parameters of the snow should be observable. Zwally (1977) correlated snow particle size with observed emissivity and used these data to calculate the accumulation rate at a few select areas.

Our method of inverting for accumulation rate is an extension of Zwally's work; undetermined coefficients in a theoretical equation relating emissivity to snow accumulation rate and temperature are fitted to *in situ* measurements in a least-squares sense. We then generate new accumulation-rate maps on a second pass using these coefficients, the observed emissivity, and the ten-meter temperature. These derived maps will, on the average, resemble the ground-truth accumulation-rate maps which served as the data base, but they may differ in specific areas. To the extent that the theoretical expressions for snow emissivity are valid, such maps may be used to refine the *in situ* data and to highlight areas where the two techniques differ.

THE SATELLITE DATA

The Scanning Microwave Spectrometer (SCAMS) on the Nimbus-6 satellite continuously

maps the Earth at 22.235, 31.65, 52.85, 53.85, and 55.45 GHz (Staelin and others, 1977). The latter three frequencies are used to probe the atmospheric temperature profile (Staelin, 1969). The 22 and 31 GHz frequencies map the Earth's surface at nadir and seven other angles; the spatial resolution near nadir is *c.* 145 km. Since this paper considers only nadir data, one-week averages are necessary to map the whole globe.

In order to analyze microwave radiometric data effectively, an accurate description of the snow's temperature profile is required. Data given by Lettau (1971) indicate that the temperature T at any depth z and time t can be approximated as

$$T(z, t) = T_{10} + T_1(z, t) \exp(-fz). \quad (1)$$

The temperature at ten meters depth, designated here as T_{10} , is assumed to be equal to the mean seasonal surface temperature. $T_1(z, t)$ is the difference between the physical temperature at depth z and T_{10} at time t , and f is the decay constant. From Lettau's Antarctic data, it appears that $T_1(0, t)$ is zero in late November; $T_1(z, t)$ is at that season only weakly dependent on z , with a maximum of approximately 5 K occurring between 2 to 3 m below the surface.

THEORY

We ignore minor atmospheric effects (Kunzi and others, 1976) and solve for snow accumulation rate by first finding a non-linear equation for brightness temperature T_b as a function of absorption and scattering coefficients. The absorption coefficient K_a is a function of the instantaneous physical temperature $T(z, t)$ of the firn while the scattering coefficient K_s is related to the area's average physical temperature T_{10} and the long-term accumulation rate A . We then use a limited set of Antarctic brightness temperature data to determine two unknown constants in this equation via regression against the known accumulation rates and firn temperatures. Finally, we use these constants in our non-linear equation to produce maps for accumulation rate in both Antarctica and Greenland using our nadir 31 GHz data.

For these inversions, we use data from 23–30 November 1975; as discussed previously the surface temperature $T(0, t)$ at this season is approximately equal to T_{10} . Moreover, numerical analysis of sample temperature profiles for this season given by Lettau (1971) and Zwally (1977) indicates that the theoretical brightness temperature varies only two or three degrees due to variations in the temperature gradient; our model suggests that natural variations in the accumulation rate over Antarctica cause much greater variations than this in the brightness temperature. Thus, we will ignore the temperature gradient and assume that $T(z, t) = T_{10}$. This is in contrast to data from January and September where the temperature gradient causes both a change in the absolute brightness temperature (warmer in summer and colder in winter) and a definite difference in the frequency response (Kunzi and others, 1976); 31 GHz observations penetrate less deeply into the snow than 22 GHz observations and hence follow seasonal changes more closely. The penetration depth at 22 GHz is on the order of a few meters.

The non-linear equation for T_b that we used is the equation of radiative transfer for a small scattering-to-absorption ratio (Zwally, 1977). If we characterize the snow at each geographic point as having a constant absorption coefficient K_a (nepers/meter) and a scattering coefficient K_s (nepers/meter) which increases linearly with depth z ($K_s = Kz$), we find:

$$T_b = T_{10} Q \left[\frac{K_a}{\sqrt{2K}} \right] \quad (2)$$

where

$$Q(x) = \sqrt{\pi x} \exp(x^2) [1 - \phi(x)] \quad (3)$$

and $\phi(x)$ is the standard error function.

Analysis by Kunzi and others (1976) indicates that the variation of the absorption coefficient K_a with temperature is principally due to changes in ϵ'' , the imaginary part of the dielectric constant; they report that at 31 GHz $\epsilon'' \approx 6.3 \times 10^{-4}$ at 256 K and $\approx 3.0 \times 10^{-4}$ at 213 K. We assume a linear relation between ϵ'' and T_{10} (Kunzi and others, 1976) and approximate K_a as

$$K_a = 4.5 \times 10^{-3} \nu (1 + 0.026 [T_{10} - 213]) \quad (\text{nepers/m}) \quad (4)$$

where the frequency ν is measured in GHz.

Accumulation rate is introduced by assuming that K_s is linearly proportional to the volume of a single snow grain, which is an empirically known function of time and temperature (Gow, 1969). This assumption is consistent with Rayleigh scattering from single spherical crystals since the amount of radiation scattered by a single crystal is then proportional to r^6 while the number of crystals per unit volume is proportional to $1/r^3$. Our linear relation between K_s and snow grain volume is also consistent with a model based on a one-dimensional stratified medium with fluctuations in the dielectric constant as a function of depth (Tsang and Kong, 1975, 1976) if the variance of the fluctuations of the dielectric constant increases at the same rate as the volume of the individual crystals. This latter model is to be preferred because the fourth-power dependence on frequency expected for Rayleigh scattering is not observed. The observed dependence is more nearly second-power, which is consistent with scattering by one-dimensional layering.

K_s can then be related to depth z , accumulation rate A (g/cm^2 year), snow density ρ_0 (g/cm^3), and ten-meter temperature T_{10} (K) by

$$K_s = C_1 \frac{z\rho_0}{A} \exp(-C_2/T_{10}). \quad (5)$$

C_1 and C_2 are undetermined positive coefficients and the snow density ρ_0 is assumed to be constant with depth.

By combining Equations (2), (4), and (5), we obtain the desired relation between brightness temperature T_b , ten-meter temperature T_{10} , and the accumulation rate A :

$$\frac{T_b}{T_{10}} = Q([C^2(T_{10})AK_1 \exp(K_2/T_{10})]^{1/2}) \quad (6)$$

where $C(T_{10})$ embodies the temperature dependence of the absorption coefficient at 31 GHz and is given by

$$C(T_{10}) = 1 + 0.026(T_{10} - 213). \quad (7)$$

The constants K_1 and K_2 are determined by the regression procedures of the next section.

EXPERIMENTAL RESULTS

Maps of snow accumulation rate were derived from satellite radiometric data for approximately 300 points uniformly spread over Antarctica for which values of ten-meter temperature T_{10} and snow accumulation rate A are known (Bentley and others, 1964; Frisrup, 1966, p. 230 and 234); these data are fairly accurate and widespread. The data were separated into eight subgroups which individually span a physical temperature T_{10} of five degrees. Linear regression analysis was applied for each subgroup to observed values of emissivity at 31 GHz and ground-truth snow accumulation rates; repetition of this process yielded for each subgroup the best value of $K_1 \exp(K_2/T_{10})$, as defined in Equation (6), which minimized the residual errors. Then these values of $K_1 \exp(K_2/T_{10})$ were analyzed as a function of T_{10} to find the optimum values of K_1 and K_2 ; the best values were $K_1 = 6 \times 10^{-12}$ and $K_2 = 5200$.

Two experiments were performed to check the validity of our model. First, a map of Antarctic snow accumulation rate was derived from Equation (5) and the observed microwave

emissivity and physical ten-meter temperature data. We assume that the ten-meter temperature maps are more accurate than ground-truth accumulation-rate maps since ten-meter temperature observations require only one visit to the desired site; snow accumulation rates are much harder to determine (Bentley and others, 1964). This experiment used the same 300 points originally used in the regression analysis; it determined whether the confidence level given to our coefficients was justified and whether the two degrees of freedom given by K_1 and K_2 are adequate to explain the variations in brightness temperature. Our second experiment was the application of our model with its previously determined coefficients to 80 points in Greenland; "hidden variables" in the Antarctic data should become apparent in this test.

Figures 1 and 2 compare the geographic contours of snow accumulation rate in Antarctica measured by ground observation with that predicted from 31 GHz data. (Intersecting contour lines on the maps are due to the finite resolution of the data points.) Interesting similarities and disagreements between the radiometric and the ground-truth data are noted. First, both the banded structure of the accumulation-rate trends in East Antarctica (between long. 0° and 120° E.) and the two patches of low accumulation rate in the lat. 77° – 79° S., long. 120° E. and lat. 77° – 79° S., long. 30° E. regions exist in the two maps. The areas of very high accumulation rate of West Antarctica and the area of relatively low accumulation rate at lat. 77° – 79° S., long. 120° – 150° W., are likewise observed in both maps. This latter region is significant, since a low-temperature area of roughly the same shape occurs at approximately lat. 77° – 79° S., long. 100° W. If we had erroneously been observing the effects of the temperature contours instead of

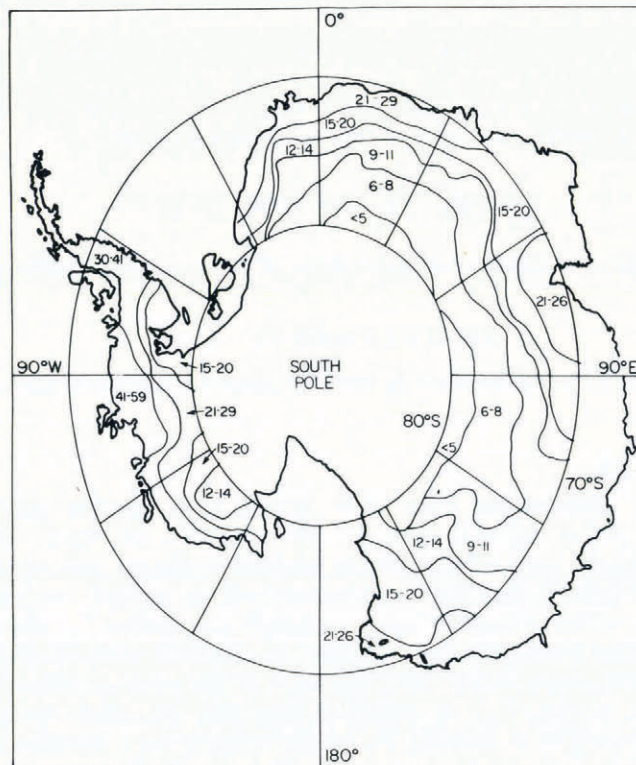


Fig. 1. Ground-truth accumulation-rate map for Antarctica (elliptical projection). Accumulation rates are measured in g/cm^2 year. Intersecting contour lines are due to the finite resolution of the data points.

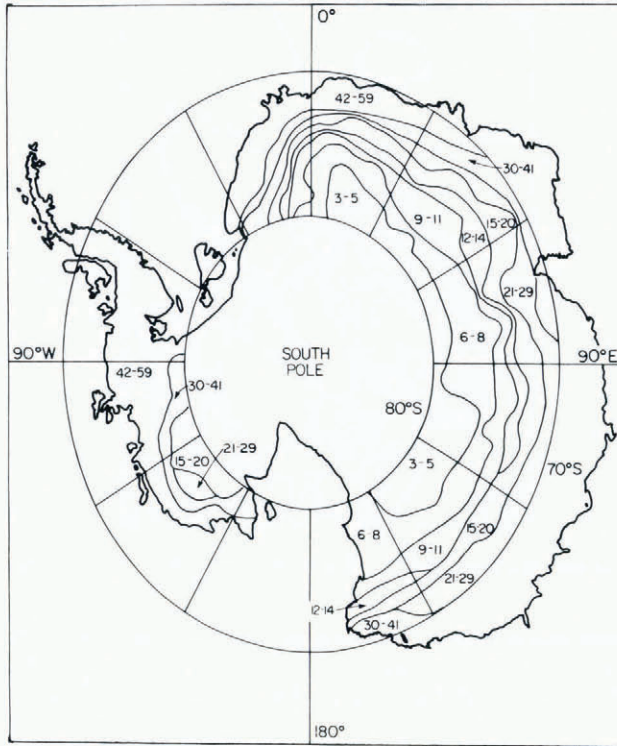


Fig. 2. Accumulation rates (g/cm^2 year) in Antarctica based on 31 GHz emissivities.

accumulation-rate trends, the gradients on the accumulation-rate maps would have been shifted to the east.

However, in some areas, the ground-truth data differ from our results. The ground-truth accumulation-rate map (Bentley and others, 1964) indicates a wedge-shaped contour of approximately $12\text{--}20\text{ g}/\text{cm}^2$ year in the region of lat. $70^\circ\text{--}80^\circ\text{ S}$., long. 150° E . that does not follow the microwave band pattern. Moreover, a statistical study of the predicted and actual accumulation rates indicates that the data divide into two populations. The first group contains approximately 230 points which vary from $3\text{ g}/\text{cm}^2$ year to $75\text{ g}/\text{cm}^2$ year with a mean value of $13\text{ g}/\text{cm}^2$ year; the root-mean-square accuracy of our best-fit data was $6\text{ g}/\text{cm}^2$ year. The second population with 55 points has accumulation rates from 8 to $58\text{ g}/\text{cm}^2$ year with an average accumulation rate of $24\text{ g}/\text{cm}^2$ year; the mean value of the error is $31\text{ g}/\text{cm}^2$ year and its root-mean-square variation is $16\text{ g}/\text{cm}^2$ year. The second, more anomalous population falls into two geographic areas; we retrieve excessively high accumulation rates at lat. $77^\circ\text{--}79^\circ\text{ S}$., long. 20° W .– 40° E . and lat. $73^\circ\text{--}76^\circ\text{ S}$., long. $60^\circ\text{--}90^\circ\text{ W}$.; the total area comprises *c.* 20% of the Antarctic region. This discrepancy may indicate substructure is present in the firn of this area for which our model has not accounted. If accumulation rates of Bentley and others (1964) are accurate, then the firn in this area is more emissive and correspondingly exhibits less scattering than expected. One hypothesis is that thermal cycling near the melting point has caused the aggregation of individual ice crystals in such a manner that scattering has diminished. Further study of data from these anomalous areas is warranted.

The Greenland analysis is even more successful than that for Antarctica, as can be seen by comparing Figure 3 (ground-truth data) with Figure 4 (radiometric data). Although the

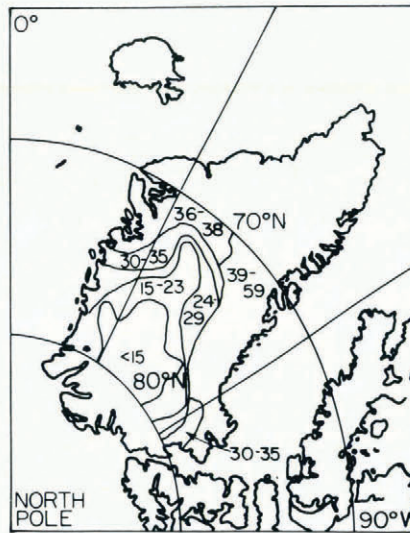


Fig. 3. Ground-truth accumulation-rate map for Greenland. Accumulation rate is measured in g/cm^2 year.

contours of snow accumulation rate in the two maps are essentially the same, the $15 \text{ g}/\text{cm}^2$ year area in the northern latitudes of Greenland in Figure 3 is resolved into the 9, 12, and $15 \text{ g}/\text{cm}^2$ year contours of Figure 4. Ignoring this area, for which accurate surface data were unavailable, the average snow accumulation rate was $29 \text{ g}/\text{cm}^2$ year for 64 points (ranging from 15 to $70 \text{ g}/\text{cm}^2$ year); our predictions had a root-mean-square error of $7 \text{ g}/\text{cm}^2$ year. It must be emphasized that the coefficients K_1 and K_2 are derived solely from the Antarctic measurements and therefore the Greenland maps represent an apparently successful and independent test of our procedures.

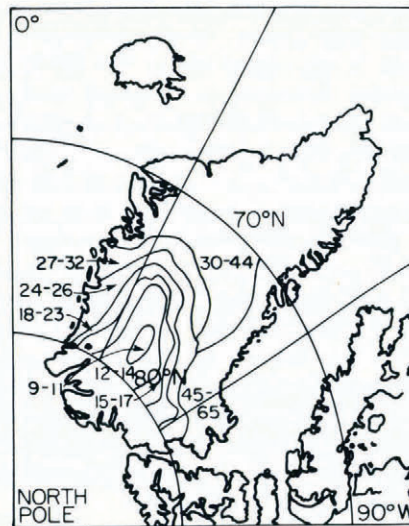


Fig. 4. Accumulation rates (g/cm^2 year) in Greenland based on 31 GHz emissivities.

The identical procedure can be followed for the 22 GHz observations. K_1 and K_2 are derived by the same regression analysis; the best fit is $K_1 = 2.55 \times 10^{-10}$ and $K_2 = 4.441$. Contours over Antarctica and Greenland similar to the 31 GHz data have been produced from the 22 GHz data.

SUMMARY AND CONCLUSIONS

A theoretical equation relating the accumulation rate, temperature, and emissivity of firn is derived and used to generate accumulation-rate maps. Coefficients derived from Antarctic data are shown to be applicable to Greenland. The present analysis is limited by the narrow range of microwave frequencies which were used in the Nimbus-6 experiment. It is expected that the Nimbus-7 SMMR experiment, with five usable frequencies at 7, 11, 18, 21, and 37 GHz, will provide much greater resolution of parameters for both dry and wet snow.

ACKNOWLEDGEMENT

This work was supported by NASA Contract NASA5-21980.

MS. received 22 May 1979 and in revised form 8 September 1980

REFERENCES

- Bentley, C. R., and others. 1964. Physical characteristics of the Antarctic ice sheet, by C. R. Bentley, R. L. Cameron, C. [B. B.] Bull, K. Kojima, and A. J. Gow. *Antarctic Map Folio Series* (New York, American Geographical Society), Folio 2.
- Chang, A. T. C., and others. 1976. Microwave emission from snow and glacier ice, by [A.] T. C. Chang, P. Gloersen, T. [J.] Schmugge, T. T. Wilheit, and H. J. Zwally. *Journal of Glaciology*, Vol. 16, No. 74, p. 23-39.
- Fisher, A. D. 1977. A model for microwave intensity propagation in an inhomogeneous medium. *IEEE Transactions on Antennas and Propagation*, Vol. AP-25, No. 6, p. 876-82.
- Fristrup, B. 1966. *The Greenland ice cap*. København, Rhodos.
- Gow, A. J. 1969. On the rates of growth of grains and crystals in South Polar firn. *Journal of Glaciology*, Vol. 8, No. 53, p. 241-52.
- Kunzi, K. F., and others. 1976. Snow and ice surfaces measured by the Nimbus 5 microwave spectrometer, [by] K. F. Kunzi, A. D. Fisher and D. H. Staelin, J. W. Waters. *Journal of Geophysical Research*, Vol. 81, No. 27, p. 4965-80.
- Lettau, H. 1971. Antarctic atmosphere as a test tube for meteorological theories. (In Quam, L. O., ed. *Research in the Antarctic. A symposium presented at the Dallas meeting of the American Association for the Advancement of Science—December, 1968*. Washington, D.C., American Association for the Advancement of Science, p. 443-75. (Publication No. 93.))
- Staelin, D. H. 1969. Passive remote sensing at microwave wavelengths. *Proceedings of the IEEE*, Vol. 57, No. 4, p. 427-39.
- Staelin, D. H., and others. 1977. Microwave spectroscopic imagery of the Earth, by D. H. Staelin, P. W. Rosenkranz, F. T. Barath, E. J. Johnston, and J. W. Waters. *Science*, Vol. 197, No. 4307, p. 991-93.
- Tsang, L., and Kong, J. A. 1975. The brightness temperature of a half-space random medium with nonuniform temperature profile. *Radio Science*, Vol. 10, No. 12, p. 1025-33.
- Tsang, L., and Kong, J. A. 1976. Thermal microwave emission from half-space random media. *Radio Science*, Vol. 11, No. 7, p. 599-609.
- Tsang, L., and Kong, J. A. 1977. Theory for thermal microwave emission from a bounded medium containing spherical scatterers. *Journal of Applied Physics*, Vol. 48, No. 8, p. 3593-99.
- Zwally, H. J. 1977. Microwave emissivity and accumulation rate of polar firn. *Journal of Glaciology*, Vol. 18, No. 79, p. 195-215.